Sergi, Claudia; Sarasini, Fabrizio; Russo, Pietro; Vitiello, Libera; Barbero, Enrique; Sánchez-Sáez, Sonia; Tirillò, Jacopo. (2022). Effect of temperature on the low-velocity impact response of environmentally friendly cork sandwich structures. *Journal of Sandwich Structures and Materials*, (2022), 24(2), pp.: 1099-1121.

DOI: https://doi.org/10.1177%2F10996362211035421

# EFFECT OF TEMPERATURE ON THE LOW-VELOCITY IMPACT RESPONSE OF ENVIRONMENTALLY FRIENDLY CORK SANDWICH STRUCTURES

Claudia Sergi[1,4*], Fabrizio Sarasini[1], Pietro Russo[2], Libera Vitiello[3], Enrique Barbero[4], Sonia Sanchez-Saez[4], Jacopo Tirillò[1]

[1] Department of Chemical Engineering Materials Environment, Sapienza Università di Roma and UdR INSTM, Italy

[2] Institute for Polymers, Composites and Biomaterials, National Research Council, Pozzuoli, Naples, Italy

[3] Department of Chemical, Materials and Production Engineering, University of Naples Federico II

[4] Department of Continuum Mechanics and Structural Analysis, Universidad Carlos III de Madrid, Spain

*Corresponding author: claudia.sergi@uniroma1.it

**Keywords**: Agglomerated Cork, PVC foam, Sandwich structures, Basalt, Flax, Low velocity impact, Temperature

**ABSTRACT**

Impact events are common in every-day life and can severely compromise the integrity and reliability of high-performing structures such as sandwich composites that are widespread in different industrial fields. Considering their susceptibility to impact damage and the environmental issues connected with their exploitation of synthetic materials, the present work aims to propose a bio-based sandwich structure with an agglomerated cork core and a flax/basalt intraply fabric as skin reinforcement and to address its main weakness, i.e. its impact response. In-service properties are influenced by temperature, therefore the effect of high (60 °C) and low (-40 °C) temperatures on the impact behavior of the proposed structures was investigated and a suitable comparison with traditional (polyvinyl chloride) (PVC) foams was provided. The results highlighted the embrittlement effect of decreasing temperature on the impact resistance of the sole cores and skins and of the overall structures with a reduction in the perforation energy that shifted, in the last case, from 50-60 J at – 40 °C up to more than 180 J at 60 °C. A maleic anhydride coupling agent in the skins hindered fundamental energy dissipation mechanisms such as matrix plasticization, determining a reduction in the perforation threshold of all composites. In particular, neat polypropylene (PP) skins displayed a perforation energy of 20 J higher than compatibilized (PPC) ones at 60 °C, while agglomerated cork sandwich structures at 60 °C were characterized by a perforation threshold higher of at least 50 J.

## 1 INTRODUCTION

Impact events due to tools drop, bird strikes, hailstorm, runway debris, car accidents can occur unpredictably in every-day life with detrimental effects to the mechanical performance of composites and, in particular of sandwich structures. These structures are widespread in many industrial applications thanks to their high stiffness-to-weight ratio [1]. It is the lightweight core material that makes them prone to impact damage along with the bonding between core and skins that leads to a stress concentration, resulting in a much more localized damage and premature skin failure [2,3].

In light of this weak point, many studies addressed the impact and post-impact response of different sandwich configurations to shed light on their complex damage scenario [4–7]. Xue et al. [8] tried to tailor the walls thickness and cells size of a NOMEX honeycomb to optimize both impact resistance and the lightweight design. Hazizan et al. [9] focused on 11 different sandwich configurations produced with PVC, PEI (polyetherimide) and PVC/PUR (polyurethane) as core materials and found out that the impact response of the structure strongly depends on foam core elastic properties. Other authors addressed also the damage tolerance of the sandwich structures carrying out an impact and post-impact campaign. Caprino and Teti [10] studied the impact resistance and the residual strength of sandwich panels with glass fiber skins and PVC foam cores with different densities and thickness whereas Schubel et al. [11] focused on the compression after impact behavior (CAI) of PVC foam sandwich structures with carbon/epoxy skins.

Sandwich Structures are characterized by another critical drawback, i.e. the exploitation of synthetic materials to produce the polymeric foams, the fibers and the matrices. These manufacturing processes are energy-intensive while the non-biodegradable nature of the synthetic components makes their disposal difficult. All these issues definitely contrast with the more restrictive regulations promulgated all over the world to counteract the uncontrolled environmental pollution. Considering this critical situation, the use of sustainable alternatives to the traditional synthetic components for the production of bio-based sandwich structures is highly encouraged.

Agglomerated cork proved to be a compelling bio-based core material endowed with good insulation capability and unique dimensional recovery capacity, which ensures a higher dimensional stability to the sandwich structure produced with it. These features combined with lightness, biodegradability, low permeability to liquid

and gases and fire retardant capability make agglomerated cork a valid alternative to common synthetic foams [12,13]. Natural fibers such as such as flax, hemp and jute can be used as logical substitutes of glass fibers in skin reinforcement, because they are cheap, abundant, and biodegradable with suitable specific mechanical properties[14]. Unfortunately, the mechanical properties of resulting composites have often disappointed the expectations due to poor Fiber/matrix interfacial adhesion, thus promoting the rise of natural fibers of mineral origin, i.e. basalt. It is characterized by mechanical properties perfectly comparable, and in some cases higher, than E-glass fibers ones. Despite its non-biodegradability, it provides many advantages when compared to glass fibers: a reduction of energy and chemicals consumption in the production process [15], reduced health risks, an easier recyclability of thermoplastic composites thanks to a lower reduction in fibers length ensuring higher residual mechanical properties [16] and an easier recovery of the fibers at the end of laminate life-cycle. Thanks to the higher melting temperature it is possible to recover them by matrix pyrolysis and partially restoring the mechanical properties through chemical treatments [17]

This environmental awareness encouraged the investigation of the impact and post-impact behavior of many bio-based and semi bio-based sandwich configurations. Baran et al. [18] studied the bending, impact and bending after impact response of glass/epoxy sandwich structures with a balsa wood core and compared their performance with the ones of styrene acrylonitrile (SAN) and polyethylene terephthalate (PET) cored structures. It was found out that balsa wood experienced the lowest decrease in initial bending stiffness, i.e. 30.5 %, with respect to SAN (35.2 %) and PET (55.6 %). Similar works were proposed by Atas and Sevim [19] who addressed the impact response of glass/epoxy sandwich structures with PVC foam and balsa wood cores and by Daniel et al. [20] who reviewed the impact and post-impact response of glass and carbon/epoxy sandwich structures always with PVC foam and balsa wood cores.

Moving to agglomerated cork, Arteiro et al. [21] compared the impact response of its sandwich structures with glass fibers skins with the one of PVC, PUR and polymethacrylamide (PMI) structures. Wang et al. [22] focused on aluminum face sheet sandwich panels produced with agglomerated cork, balsa wood, polystyrene (PS) and polypropylene (PP) honeycomb as core materials and Castro et al. [23] studied the bending and impact behavior of agglomerated cork, PMI and PVC carbon/epoxy structures. A further step was taken by Hacheman et al. [24] who proposed environmental-friendlier sandwich structures produced with an agglomerated cork core and with jute fibers reinforced skins. The post-impact response of agglomerated cork with an epoxy resin

and PMI sandwich structures was addressed by Silva et al. [25] who found out a higher damage tolerance of cork composites when compared with PMI ones.

This literature survey highlighted the lack of studies on the effect of temperature on the low-velocity impact response of cork-based sandwich structures. To bridge this gap, the present work aims to study the effect of a wide range of temperatures, i.e. low (-40 °C), room and high (60 °C) temperatures, on the low-velocity impact performance of agglomerated cork core sandwich structures with intraply flax/basalt hybrid polypropylene skins. The use of a hybrid fabric allows to synergistically combine the high mechanical properties of basalt fibers with the low density and biodegradability of flax fibers. To fully understand the impact response of the proposed structures, the low-velocity impact campaign as a function of temperature was performed at first on the single components of the panel, i.e. cores and skins, and only at a later time on the overall structure. Three agglomerated corks with different densities were selected to study the effect of this parameter on the sole core response and the results obtained were suitably compared with the ones of three traditional PVC foams characterized by the same densities and employed as benchmark. Based upon these first results, two agglomerated corks and one PVC foam were selected to produce the overall sandwich structures. The polypropylene skins were produced with and without a maleic anhydride coupling agent to address the effect of this component on the dynamic behavior of the single laminates and of the sandwich panels.

## 2 MATERIALS AND METHODS

### *2.1 Materials*

The first step of the experimental campaign, i.e. the one on the sole core, was carried out on six different core materials: three agglomerated corks with different densities and three PVC foams characterized by the same densities of the natural cores selected. The employment of these well-established polymeric foams allows to disclose the points of strength and weakness of the bio-based cores proposed. NL10 (140 kg/m$^3$), NL20 (200 kg/m$^3$) and NL25 (250 kg/m$^3$) agglomerated cork planks with a thickness of 15 mm were supplied by Amorim Cork Composites®, while Divinycell HP130 (130 kg/m$^3$), Divinycell HP200 (200 kg/m$^3$) and Divinycell HP250 (250 kg/m$^3$) PVC closed cells foam plates, always with a 15 mm thickness, were provided by Diab®.

Polypropylene (PP) skins produced by hot compression molding were selected for the present work considering the improved ductility of thermoplastic matrices with respect to brittle thermosetting ones.

Bormod™ HF955MO supplied by Borealis AG and Polybond® 3000 (maleic anhydride content of 1.2 wt% and a MFI at 190 °C of 405 g/10min) supplied by Chemtura Corporation are the neat polypropylene and the coupling agent employed, respectively. Compatibilized skins (PPC) were obtained adding 2 wt% of coupling agent to the neat PP by means of a corotating twin screw extruder Collin Teach-Line® ZK25T working with a temperature profile of 180 °C - 190 °C - 205 °C - 195 °C -185 °C and a 60 rpm screw speed. The polymer films (thickness of 75-80 μm) for hot compression molding were manufactured with a flat film extrusion line Teach-Line® E 20 T supplied by Collin GmbH and equipped with a calender CR72T operating with a screw speed of 55 rpm and a temperature profile of 180 °C - 190 °C - 200 °C - 190 °C -185 °C. The skins were reinforced with an intraply flax/basalt hybrid fabric, i.e. LINCORE® HF T2 360, provided by Depestele Group which is a balanced twill 2/2 fabric with 50 wt% of basalt and 50 wt% of flax and with an areal density of 360 g/m$^2$. P400E supplied by Collin GmbH is the molding machine employed to hot compress the skins produced applying the film stacking technique and alternating a film of matrix and a ply of fabric for a total number of four twill layers and an overall thickness of 2.2 ± 0.1 mm for PP and 2.1 ± 0.1 mm for PPC composites. The manufacturing process was carried out according to the optimized temperature-pressure cycle reported in Figure S1 of supplementary materials.

Based upon the results on cores, NL10 and NL25 agglomerated corks and HP130 foam were selected as core material to produce PP and PPC sandwich structures. The use of NL10 and HP130 provides a direct comparison between structures with the same weight, whereas the employment of NL25 and HP130 allows to compare the agglomerated cork and the polymeric foam with the closest mechanical behavior. Sandwich structures were produced by bonding the core and the skins with the bicomponent epoxy resin Elan-tech® ADH 46.46 by Elantas. The panels were produced by a two-step process gluing the first skin and waiting 24 hours to ensure resin complete curing before gluing the second one. The overall structure was placed under a constant load during the curing process to promote core-skin adhesion and the glued skin was placed below the core to facilitate resin excess removal avoiding gravity-driven percolation in the core. Sandwich panels produced with PP skins were characterized by an overall thickness of 19.4 ± 0.3 mm while the ones produced with PPC skins by an overall thickness of 19.2 ± 0.3 mm.

*2.2 Low-velocity impact tests*

Sole cores, skins and the overall sandwich structures were impacted in accordance with ASTM D7136. Rectangular specimens with a length of 150 mm and a width of 100 mm were suitably tested clamping the samples to the support (unsupported area of 75 x 125 mm) through four manual handles placed at the corners of the samples. Considering the soft nature of cork, an aluminum frame with outer dimensions coinciding with sample ones, inner dimensions coinciding with rectangular hole ones and a thickness of 0.4 mm was placed between the handles and the specimens to prevent local indentation. To keep constant the boundary conditions, the frame was employed to test skins and sandwich panels, too. A hemispherical impactor with a diameter of 12.7 mm and an overall mass of 6.763 kg for core and skins and 12.055 kg for sandwich structures was employed.

The perforation energy of each component was identified employing the energy profile diagram technique [26]. Some exemplifying curves for core, skin and sandwich structures perforation energy identification are shown in Figure 1. The diagram is characterized by three regions: no penetration (I), penetration (II) and perforation (III). The first region is characterized by a parabolic shape and is located below the equal energy line because the energy dissipated by the specimen is lower than impact one leading to impactor rebound. In the penetration region (II) the curve coincides with equal energy line because the specimen dissipates all impact energy and the impactor sticks into the sample. This region extends up to sample perforation and its extent varies significantly as a function of the material under study, degenerating in a point in the most critic cases [27]. In the third region, the dissipated energy is constant and coincides with material perforation threshold which is the maximum energy that the material is able to absorb. In this region a certain dispersion in the absorbed energy could be found due to the randomness of the damage caused by the impactor. Once identified the perforation energy, each core material, each skin type and each sandwich configuration were tested at 75 %, 50 % and 25 % of this value evaluating maximum force, maximum displacement and percentage absorbed energy, i.e. the ratio between the absorbed and the impact energy.

This procedure was employed for all impact tests: room temperature, low (-40 °C) and high (60 °C) temperatures. These operating conditions were achieved through a drop weight tower equipped with a climatic chamber provided with nitrogen cooling connectors and heaters. All samples were suitably pre-conditioned for two hours at the required temperature to ensure a homogeneous temperature profile across the specimen.

Concerning the sole cores, a minimum number of five samples was tested in each condition whereas a minimum number of three samples was selected for sole skins and sandwich structures.

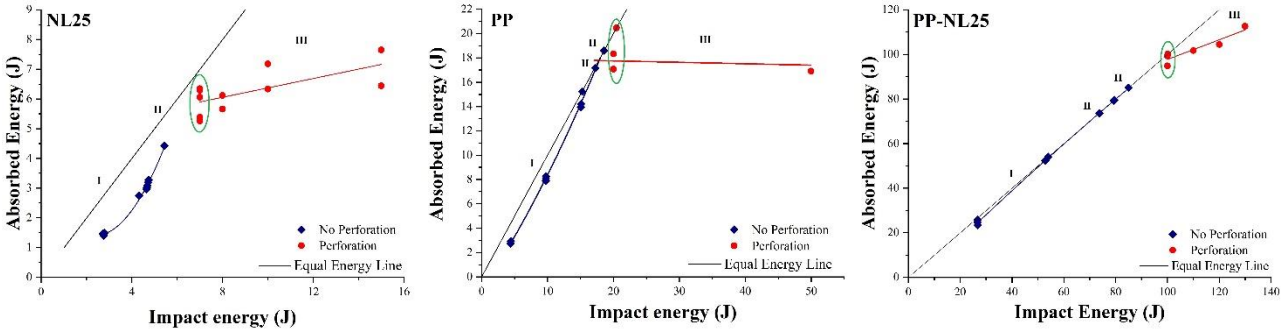


Figure 1: Exemplifying energy profile diagram for NL25 core, PP skins and PP-NL25 sandwich structures

*2.3 Post-impact analysis of the damage*

A post-impact analysis was carried out on the sole cores and on the sandwich structures to evaluate the damage extent induced by the impact. Core samples were subjected to a front and back side analysis to quantify the residual indentation depth left by the impactor and the back-crack extent, respectively. The residual indentation was evaluated through a a laser profilometer Talyscan 150 by Taylor Hobson. This investigation was performed only on PVC foams because the high recovery capacities of cork tend to cancel impactor marks after a short time from the impact. Back side analysis aimed to detect and quantify the crack produced as a consequence of the bending deformation induced by the impact. At first the cracks were made visible by local infiltration with a red paint by means of a syringe and the images were processed with the program Image J to measure crack length. Concerning sandwich structures, the damage left by the impactor in the inner parts of the panel was visually inspected by cutting the sample in two halves.

*2.4 Thermal analysis*

To support the impact results obtained in the wide range of temperatures and to disclose the actual effect of this parameter on the dynamic response of the composites skins were subjected to Differential Scanning Calorimetry (DSC) using a TA DSC 2920 calorimeter by TA Instruments. Samples were heated from -40 °C up to 200 °C and were then cooled following the same path employing a heating rate of 10 °C/min in a nitrogen atmosphere with a flow rate of 70 ml/min. Before starting the measurement, samples were hold at -40 °C for five minutes.

## 3 RESULTS AND DISCUSSION

### *3.1 Low-velocity impact response of cores*

Core materials low-velocity impact response was investigated and the perforation thresholds of each core type as a function of operating temperature are reported in Table 1. PVC foams show a constant increase in perforation energy for increasing foam density and for rising operating temperatures. Concerning foam density, an increase in this parameter leads to thicker cell walls which require a higher amount of energy to deform, collapse and cracks thus implying a higher perforation threshold of the material. Moving to temperature effect, the results obtained can be explained considering the DMA results and the resulting glass transition temperature values summarized in Table 2 [28]. Even if all polymeric foams are well below their glass transition temperature in the whole testing range and work constantly in the glassy state, their storage modulus is characterized by a slight progressive decrease for increasing temperatures and this provides a gradual mitigation of their brittle behavior. More complex is agglomerated cork scenario, where the effect of density proved to be less pronounced and the highest perforation threshold, and hence the highest impact resistance, is reached at room temperature.

Concerning density, an increase of only 1 J in the perforation energy was observed for increasing density. Even if the higher compactness of the denser planks makes samples stiffer, as confirmed by the curves in Figure S2 of supplementary materials, the weak point of agglomerated cork is cork granules - polymeric binder interface that leads to a premature detachment of samples plug thus hindering the full exploitation of cork energy absorbing capabilities. Focusing on temperature effect, all agglomerated corks suffer a reduction of 2 J in the perforation threshold when tested at 60 °C due to the progressive softening of the polyurethane binder that makes agglomerated cork even more prone to premature failure. The decrease in perforation energy at -40 °C must be ascribed to the approach of the polymeric binder to its glass transition temperature (Table 2) that causes its embrittlement thus reducing its energy absorption capacities.

Table 1: Perforation energies of the six core materials as a function of operating temperature

| Core | Perforation Energy at -40 °C (J) | Perforation Energy at Room Temperature (J) | Perforation Energy at 60 °C (J) |
|---|---|---|---|
| NL10 | 4 | 5 | 3 |
| NL20 | 6 | 6 | 4 |
| NL25 | 5 | 7 | 5 |
| HP130 | 10 | 13 | 14 |
| HP200 | 12 | 25 | 27 |
| HP250 | 15 | 30 | 34 |

Table 2: Core materials glass transition temperature [28]

| Core | Glass transition temperature (°C) |
|---|---|
| NL10 | 11.75 ± 0.78 (-40 °C polymeric binder) |
| NL20 | 10.90 ± 2.12 (-40 °C polymeric binder) |
| NL25 | 15.80 ± 1.27 (-40 °C polymeric binder) |
| HP130 | 85.40 ± 0.56 |
| HP200 | 79.80 ± 1.98 |
| HP250 | 76.80 ± 0.99 |

A deeper understanding of the low-velocity impact response of all core materials can be achieved considering the response curve at 50 % of perforation energy shown in Figure 2 and the maximum force, maximum displacement and percentage absorbed energy data reported in Figures S3 and S4 of the supplementary materials. The first outcome to point out is the embrittlement effect played by decreasing temperature on both natural and synthetic cores, underlined by the increased linear stiffness, i.e. higher initial curve slope, the progressive decrease in the maximum displacement and the general decrease in the percentage absorbed energy. The variation in sample stiffness is very pronounced in the case of agglomerated cork which features binder glass transition at -40 °C and cork glass transition at around 15 °C and is more evident for PVC at 60 °C due to the progressive approach of its glass transition region. The main differences between agglomerated cork and PVC foam response arise when maximum force evolution is considered, in fact agglomerated cork displays a decrease in this parameter for increasing temperature whereas PVC foam shows an increase. In the case of cork, this can be justified considering that its glass transition takes place between 11 °C and 16 °C as

a consequence of suberin melting [29] thus determining a sharp change in material storage modulus and implying that at -40 °C the material is working well below and at 60 °C well above this transition value. Different is PVC situation where an increase in temperature in the glassy region induces a small decrease in material brittleness allowing an easier deformation and indentation of the material and, as a consequence, an easier approach of the densification region due to cell collapse that causes the increase in maximum force. This hypothesis is corroborated by the permanent indentation depth values obtained through profilometry and reported in Figure 3 that show an increase in the damage depth left by the impactor for increasing operating temperature. Looking at PVC foams curves, a first peak force followed by a sharp drop can be recognized in the first part of the impact curve. This peak can be ascribed to the appearance of a brittle crack on the back side of the sample due to the bending deformation underwent by the material. Same type of damage is suffered by agglomerated cork, but the identification of this phenomenon on the impact curve is more complicated due to the weak interface at granules boundaries. In light of this common damage feature, an analysis of crack extension as a function of impact energy and test temperature was carried out on both core types. Figure 4 shows crack extent evolution for NL25 and HP130 and Figure 5 summarizes the crack lengths measured for all core materials in every working condition.

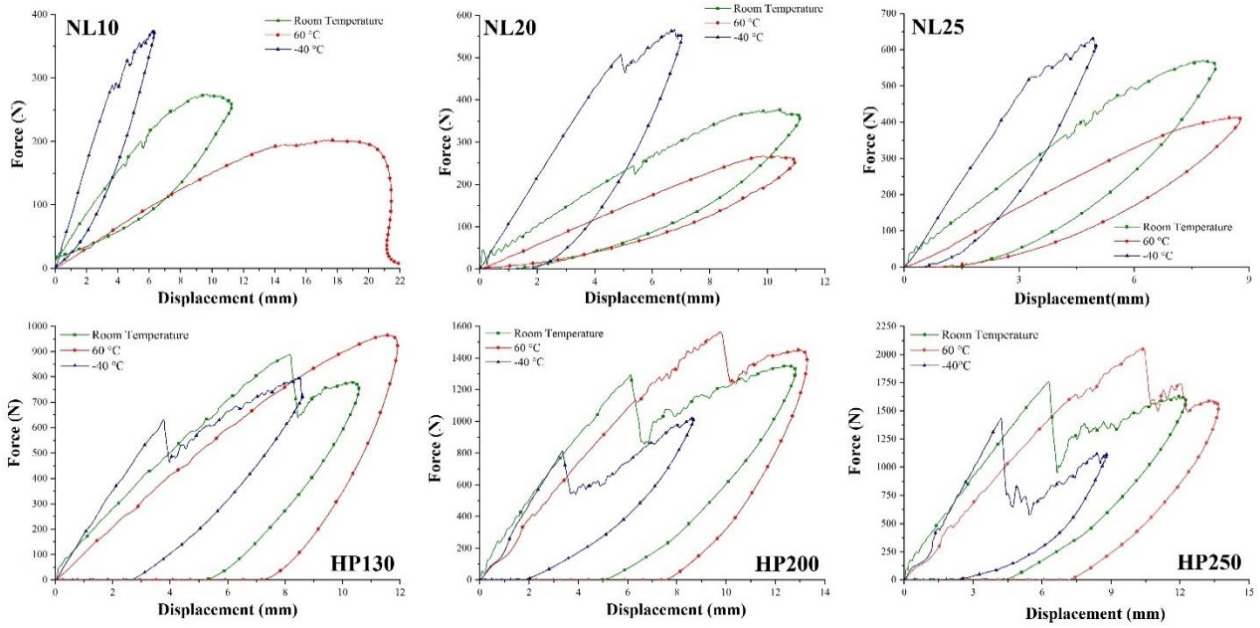


Figure 2: Agglomerated corks and PVC foams impact response curves at 50 % of perforation energy as a function of temperature

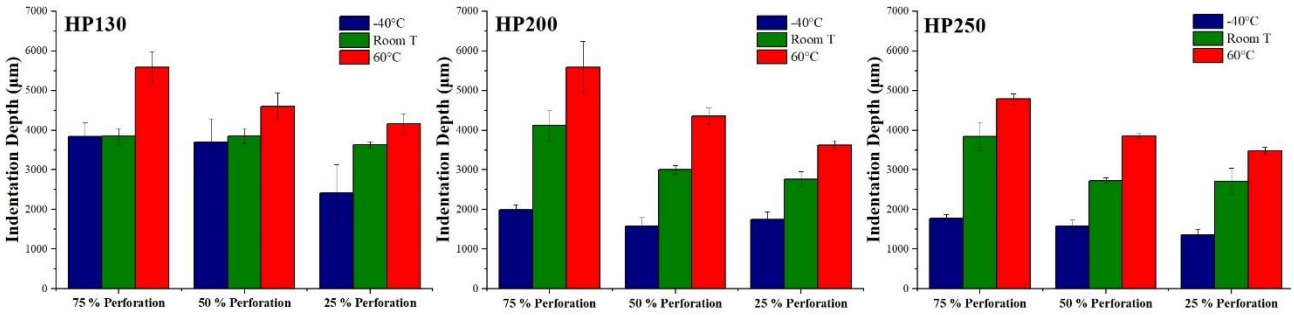


Figure 3: Permanent indentation depth of the three polymeric foams as a function of impact energy and operating temperature

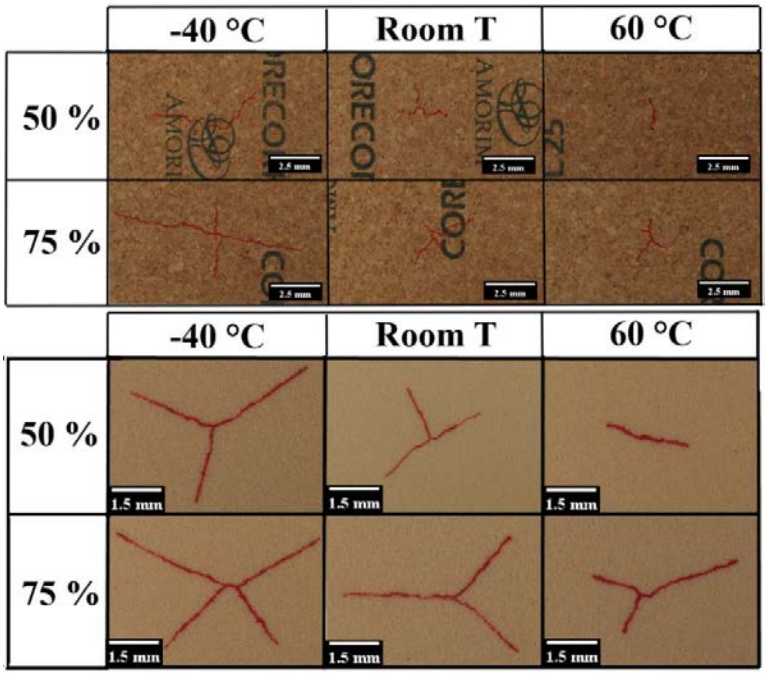


Figure 4: Crack extent evolution as a function of impact energy and temperature in NL25 and HP130

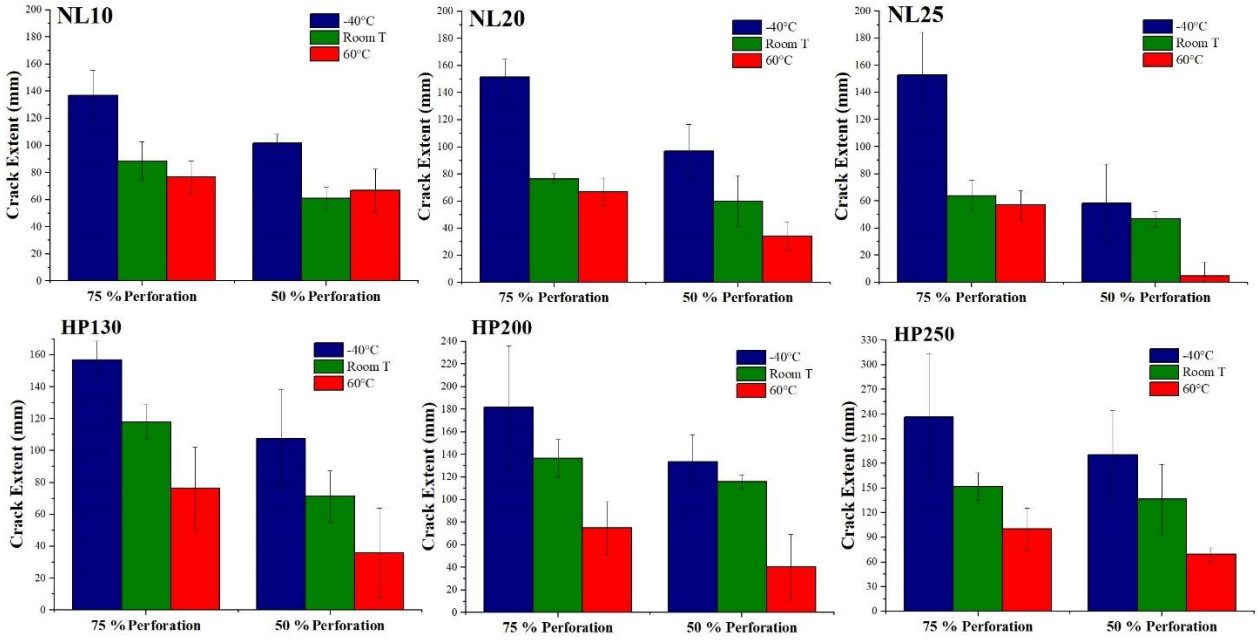


Figure 5: Crack extent as a function of impact energy and temperature for all core materials

The increase in back-side fracture for decreasing temperature proves unequivocally the embrittlement effect suffered by the core materials. The transition of cork from the viscoelastic to the glassy state at room temperature implies a reduction of cell walls deformability and hence an overloading of the polymeric binder that becomes maximum at -40 °C when the latter approaches its glass transition temperature. As further proof, the differences in crack length between 60 °C and room temperature ranges only between 10.8 % and 13 % and rise up to 35.4 %-58.3 % moving from room temperature to -40 °C for a 75 % perforation energy impact. Concerning PVC foams, the increase in crack extent is a direct consequence of the reduction in the permanent indentation already shown in Figure 3. The hindering of energy dissipation mechanisms, such as foam densification, forces the material to dissipate the impact energy through crack propagation.

*3.2 Low-velocity impact response of hybrid skins*

The low-velocity impact response of compatibilized and not compatibilized polypropylene skins was investigated as a function of operating temperature. Table 3 summarizes the perforation energy of each skin type as a function of temperature, Figure 6 shows the impact response curve at 25 % of perforation energy as a function of temperature and Figure S5 of supplementary materials reports maximum force, maximum displacement and percentage absorbed energy data for all impact conditions. Many studies already acknowledged the detrimental effect played by coupling agent on the impact response of composite laminates. Simeoli et al. [30], Sorrentino et al. [31] and Boccardi et al. [32] found out a decrease in the impact resistance of PP/glass fiber reinforced composites when fiber-matrix interface is improved with a coupling agent. Composite materials dissipate the energy of an impact through matrix and fibers breakage and delamination phenomena, but a weak fiber-matrix interface can provide for additional energy dissipation mechanisms, i.e. fibers pull out and fiber-matrix friction. They increase material impact strength preserving its integrity at higher impact energies before final failure occurs. Fibers slippage ensures a local rearrangement of the reinforcement in the matrix leaving to the latter the possibility to deform plastically thus promoting another energy dissipation mechanism. All these energy consuming phenomena are hindered in compatibilized composites where the improved fiber-matrix interface prevents fibers local rearrangements and matrix plastic deformation inducing an embrittlement effect in the material.

The present work confirms the detrimental effect played by the coupling agent on laminates impact response especially when high operating temperatures are considered. At room temperature and -40 °C, PP and PPC skins show small difference in perforation threshold, i.e. 2 J, but this gap increases at 60 °C where PP skins are characterized by a perforation energy of 20 J higher than PPC ones. At -40 °C both PP and PPC are working in the glassy state considering that PP glass transition temperature is at around -12.5 °C, as shown in the DSC thermogram in Figure S6 of supplementary materials. In this condition both laminates are characterized by a brittle behavior and matrix plastic deformation is hindered. The differences that arise between PP and PPC are limited and mainly due to fiber friction and rearrangement due to PP poor interface. At room temperature the overcoming of polypropylene glass transition temperature promotes a small increase of 3 J in both PP and PPC perforation energy, but the overall response of the laminates does not change significantly as also confirmed by sample stiffness that keeps almost unchanged as shown in the response curves in Figure 6. A clear change in skins behavior can be observed at 60 °C thanks to the exceeding of flax fibers glass transition temperature and to the fact that the matrix is working well far from its glass transition temperature being able to fully exploit plasticization phenomena. Flax glass transition takes place at around 55.5 °C and 60 °C as already acknowledged by Dong et al. [33] and by Khalfallah et al. [34]. This is also confirmed by the large drop in the DSC thermogram in Figure S6 of supplementary materials that extends up to 65 °C – 70 °C and includes moisture removal from flax fibers and flax glass transition. The improved ductility of the matrix is also confirmed by the strong reduction in laminates stiffness as observed in impact curves in Figure 6. The trigger of plasticization phenomena discloses the profound difference between PP and PPC skins, in fact the good fiber-matrix interface of compatibilized composites keeps unchanged their brittle response whereas the poor fiber-matrix interface in PP composite allows fibers rearrangement with consequent exploitation of matrix plasticization. This allows to spread the impact load over a wider area of the composite as confirmed by samples damage mode shown in Figure 7. PPC skins are characterized by a main central crack running transversally to flax fibers that proves the localization of the damage whereas PP skins display a global reaction of the whole area interested by the impact.

Table 3: Perforation energies of skin laminates as a function of operating temperature

| Skin | Perforation Energy at -40 °C (J) | Perforation Energy at Room Temperature (J) | Perforation Energy at 60 °C (J) |
|---|---|---|---|
| PP | 17 | 20 | 40 |
| PPC | 15 | 18 | 20 |

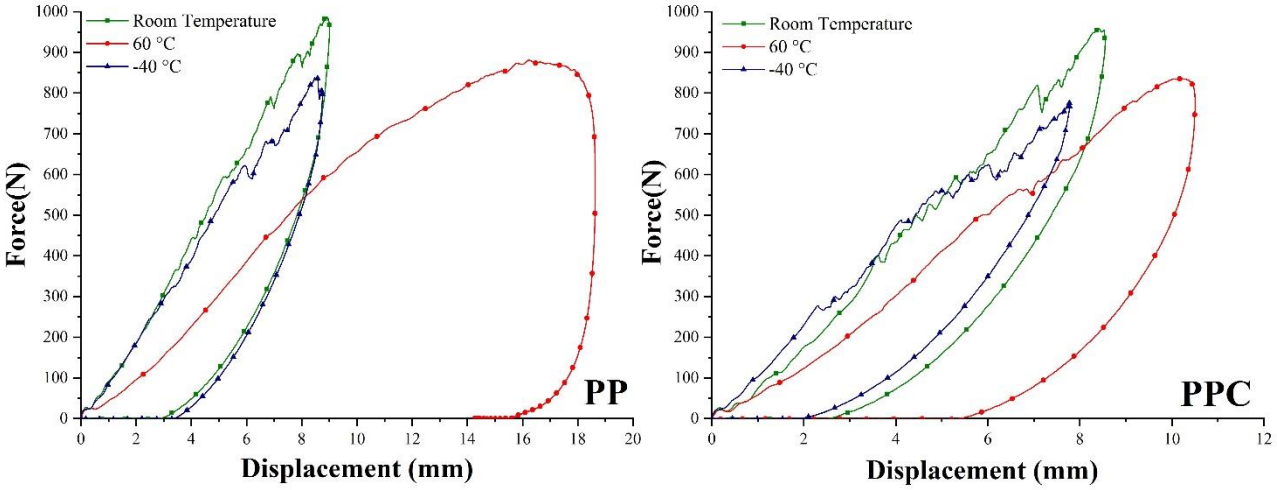


Figure 6: PP and PPC impact response curves at 25 % of perforation energy as a function of operating temperature

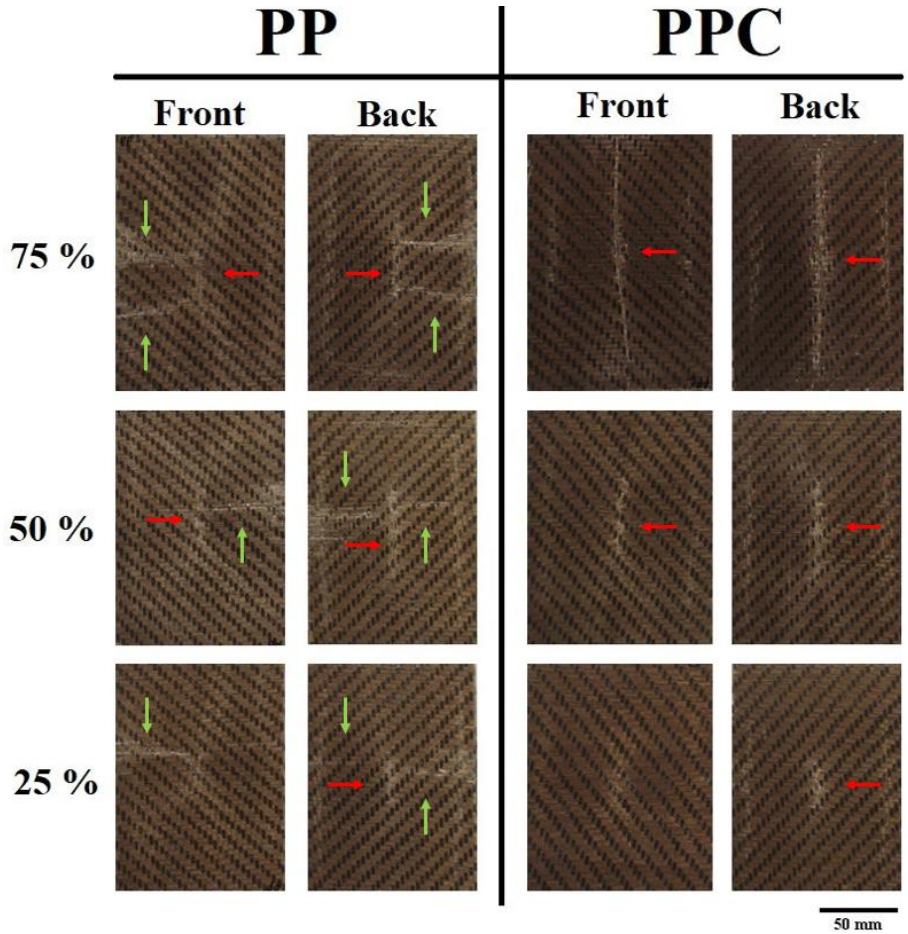


Figure 7: Damage progression in PP and PPC skins at 75 %, 50 % and 25 % of perforation energy at 60 °C. (Red arrows point the main central crack, i.e. localization of the damage; Green arrows highlight further area of deformation which emphasize a more global response of the specimen)

More information about skin low-velocity impact response can be obtained from the data presented in Figure S5 of supplementary materials. At 60 °C both PP and PPC are characterized by the highest maximum displacement and percentage absorbed energy thanks to the strong ductility acquired by the matrix that can undergo large deformations consuming a higher amount of energy especially for neat PP skins. PP skins are characterized by the highest maximum force and the lowest maximum displacement at room temperature and by the lower maximum force at -40°C. The difference in maximum displacement between room temperature and -40 °C can be explained considering that at room temperature the matrix has moved to its viscoelastic state and the material needs to deform less to dissipate the impact energy considering that the perforation thresholds are close. Concerning the peak force, it must be considered that it is reached when bending cracks occur on the bottom face of the laminate, which appears earlier at -40 °C being the samples more brittle. Moving from room temperature to 60 °C, there is a decrease in the maximum force due to the further softening of the matrix. Different is PPC situation where the increase in temperature plays a role similar to the one observed in PP, but where the good fiber-matrix interface makes the laminate behave in a brittle way even at 60 °C and hence the maximum displacement increases moving from -40 °C to room temperature where the material still behaves in a brittle way.

### *3.3 Low-velocity impact response of sandwich structures*

Based upon the obtained results, NL10, NL25 and HP130 were selected as core materials to produce the bio-based sandwich structures. Table 4 summarizes the perforation thresholds of all six sandwich configurations at room temperature and -40 °C. Results at 60 °C will be introduced later. When tested as sole cores, NL10 and NL25 display a perforation energy much lower than HP130 due to the premature detachment of cork plug induced by the poor interface between cork granules and polymeric binder. The situation changes considerably when the two natural cores are embedded in the complete structure thanks to the outer skins which prevent plug detachment and allow the full exploitation of cork energy absorbing capabilities. NL25 structures display a perforation threshold 20 J higher than HP130 ones for both PP and PPC skins and NL10 a perforation energy of 5 J higher than HP130 one for PPC skins at room temperature. This can be ascribed to the stiffer nature of HP130 structures in bending which makes hard for the impactor to bend the sample leading to a concentration of the load in a more restricted area. These results are promising in view of the achievement of performing bio-based sandwiches for applications where impact resistance is one of the key design parameters. Another

important outcome from room temperature results is that PP skins are able to provide an improved impact resistance to the sandwich structures with respect to the brittle PPC skins. All these findings are confirmed by the observation of sandwich damage progression at room temperature shown in Figure 8 for HP130 (A), NL10 (B) and NL25 (C). NL10 and NL25 structures are characterized by a conical crack damage of the core due to damage propagation through the polymeric binder and this enables to spread the impact load on a wider area of the samples. On the contrary, PVC foam panels display a more localized and concentrated damage of plugging type due to the stiffer nature of the structures that determines a higher permanent indentation with respect to agglomerated cork especially at 50 % and 75 % of perforation energy as also confirmed by the permanent indentation data shown in Figure 9. This pronounced indentation will likely imply a higher reduction in the residual flexural properties of the structures. This potentially suggests that structures with agglomerated cork cores are characterized by a higher damage tolerance especially if it is considered that PPC-HP130 and PP- and PPC-NL10 sandwiches were impacted at similar impact energies and that PP-HP130 and PPC-NL25 composites were impacted at the same impact energies. From the permanent indentation data is also possible to highlight that at 25 % of perforation energy PP sandwiches are always characterized by a higher permanent indentation than the corresponding PPC ones. This is due to the fact that all structures are still working in the elastic regime and the permanent indentation suffered by the structure depends on the stiffness of the upper skin, which is higher for PPC skins, and by the higher impact energy applied to PP structures. The situation changes at 50 % of perforation energy where the penetration of the impactor due to the collapse of the upper skin occurs. Considering the higher energy dissipation capability of neat PP skins thanks to matrix plasticization, a lower penetration of the impactor in the core is needed.

Table 4: Perforation energies of the six sandwich configurations as a function of operating temperature

| Core | Perforation Energy at -40 °C (J) | Perforation Energy at Room Temperature (J) |
|---|---|---|
| PP_NL10 | 50 | 65 |
| PPC_NL10 | 50 | 65 |
| PP_NL25 | 60 | 100 |
| PPC_NL25 | 60 | 80 |
| PP_HP130 | 50 | 80 |
| PPC_HP130 | 50 | 60 |

Moving to the low and high temperatures results, it is necessary to highlight that, if for samples tested at -40 °C it was possible to identify the perforation energy and to provide a direct comparison with room temperature results, this was not possible for samples tested at 60 °C. Indeed, the higher operating temperature led to a significant increase in the perforation threshold of agglomerated cork PP sandwiches which could not be perforated even increasing the impactor mass from 12.055 kg to 17.055 kg to reach impact energies of 170 J and 180 J, as shown in Figure S7 of supplementary materials. The strong plasticization of the matrix and the poor fiber-matrix interface allow to spread the impact load over a wider area involving a significant bending of the sample and preventing perforation. Due to the inability of reaching the perforation threshold of these composites and in order to work with the same impactor mass employed at room temperature and at -40 °C, all six sandwich configurations were tested at 130 J and at 75 %, 50 % and 25 % of this value. This value is the highest achievable with this impactor mass and actually coincides with PPC NL10 and NL25 sandwiches perforation energy. In this way it was possible to obtain a direct comparison of samples impact response being equal the impact energy.

Starting with the comparison of the results at room temperature and -40 °C, a strong reduction in the perforation threshold of all sandwich structures can be observed moving from room temperature to -40 °C looking at the data in Table 4. This significant decrease is due to the embrittlement effect suffered by the core and especially by the skins which move from the viscoelastic to the glassy state and are not able to dissipate energy through plasticization anymore. This is confirmed by the fact that at -40 °C both PP and PPC composites are characterized by the same perforation energy. This means that the hindering of matrix plastic deformation of PP skins makes them act in a brittle way as PPC skins do at all temperatures due to the improved fiber-matrix interface. Concerning core type, NL10 is able to provide the same impact resistance of HP130 not only with PPC skins, as happens at room temperature, but also with PP skins, whereas NL25 still provides a higher impact resistance with a 10 J higher perforation energy. More conclusions can be drawn from the curves shown in Figure 10 and the percentage absorbed data in Figure S8 of supplementary materials. The impact response curves show a clear embrittlement in the response of the structures that present a higher reaction force, a much lower maximum deformation and a higher initial curve slope that preempts a higher stiffness of the material.

Concerning the percentage absorbed energy, a thorough understanding of sandwich structures response requires the consideration of damage evolution at -40 °C shown in Figure S9 of supplementary materials for

HP130 (A), NL10 (B) and NL25(C). At 75 % of perforation energy, room temperature and -40 °C samples are characterized by equal absorbing capabilities because impactor penetration occurs preventing the rebound and inducing a whole absorption of the impact energy. Similar results were obtained at 50 % of perforation energy with the exception of PP-NL10 samples. They are characterized by a lower percentage absorbed energy at room temperature because the sample provides a perfectly elastic rebound without undergoing any penetration thus absorbing a lower amount of energy as also confirmed by damage progression in Figure 8. Moving to 25 % of perforation energy, where all sandwich structures respond elastically to the impact, it is possible to notice that PP skin composites at room temperature are characterized by a higher percentage absorbed energy. The viscoelastic response of the PP matrix and of the cores increases the damping capability of the structure. Focusing on the damage progression, even if NL10 and HP130 composites are characterized by the same perforation energy, HP130 structures suffer a higher localization of the damage, especially at 75 % and 50 % of perforation energy, which can severely compromise the damage tolerance and the residual mechanical properties of the structures. This is true even when comparing HP130 and NL25, even if the latter is tested at higher impact energies thanks to its higher perforation threshold.

As previously mentioned, a direct comparison of the results at 60 °C with the room temperature and -40 °C ones is not possible, but a direct comparison between the different sandwich configurations can be made and some conclusions on the effect of a higher operating temperature can be drawn. Maximum force, maximum displacement and percentage absorbed energy data at 60 °C for all sandwich configurations are reported in Figure 11. Figure S10 of supplementary materials show sandwich damage progression at 60 °C for HP130 (A), NL10 (B) and NL25 (C), respectively. The first conclusion that can be drawn is that moving from room temperature to 60 °C there is an increase in composite perforation threshold. Indeed, even if PP NL10 and NL25 perforation energy could not be detected, their impact resistance is certainly higher than room temperature one where they underwent perforation at 65 J and 100 J, respectively. This is also confirmed by PPC NL10 and NL25 composites that display a perforation energy of 130 J at 60 °C which is definitely higher than 65 J and 80 J obtained at room temperature. The improved impact resistance of these structures must be ascribed to the combination of the strong ductility acquired by the matrix, especially in the case of PP skins, and the capability of agglomerated cork to adapt to the imposed deformation involving a wider area of the samples and avoiding local stress concentrations.

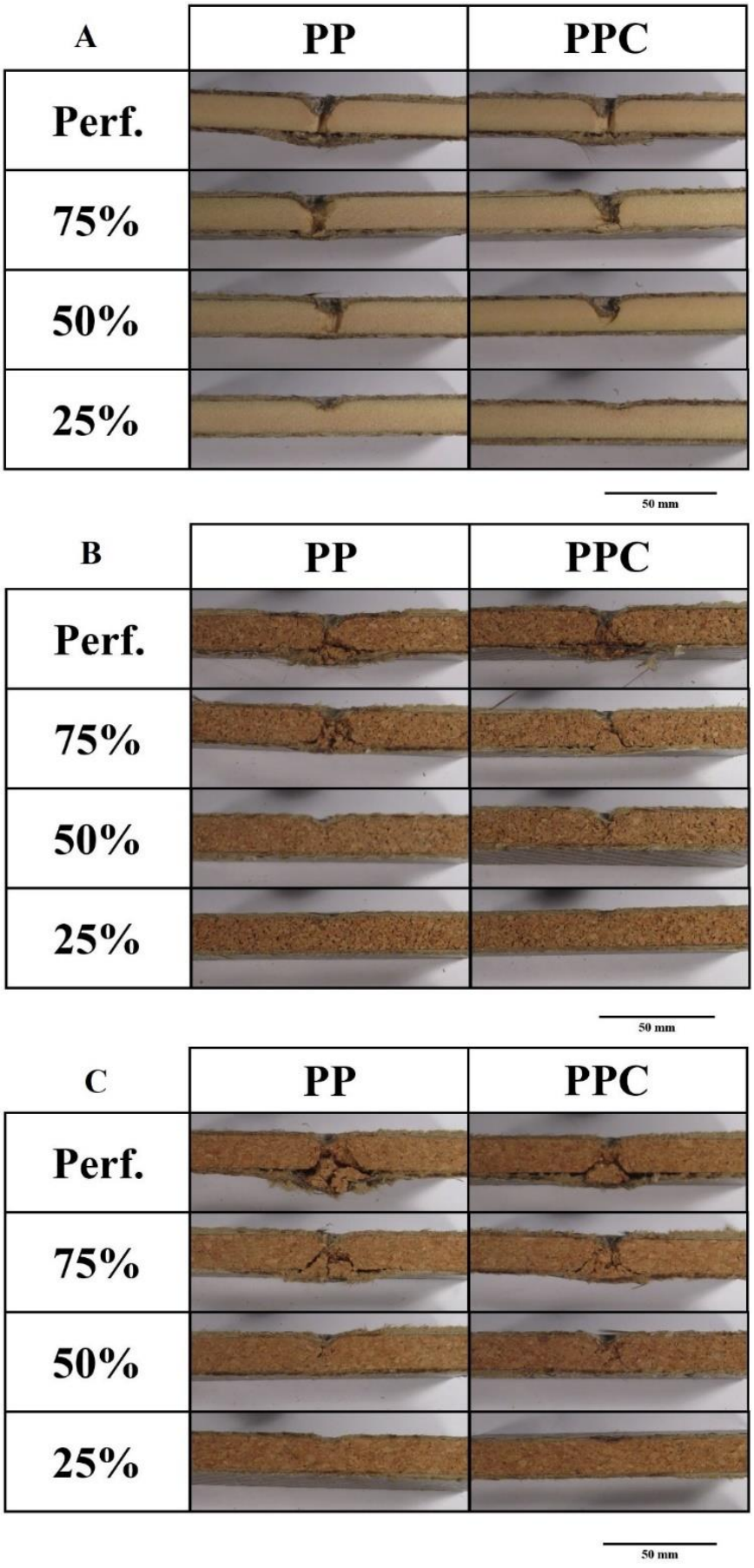


Figure 8: Damage progression in PP and PPC HP130 (A), NL10 (B) and NL25 (C) sandwich structures at room temperature as a function of impact energy

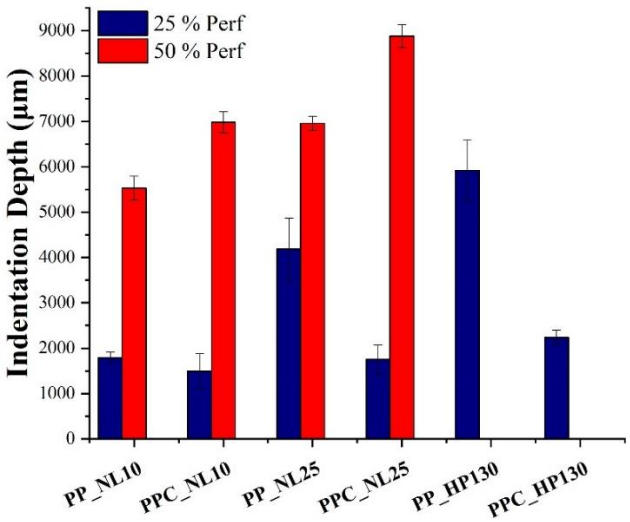


Figure 9: Permanent indentation depth of the six sandwich configurations at 25 % and 50 % of perforation threshold. HP130 50 % perforation energy data are not available due to a severe indentation not measurable with the scanning laser.

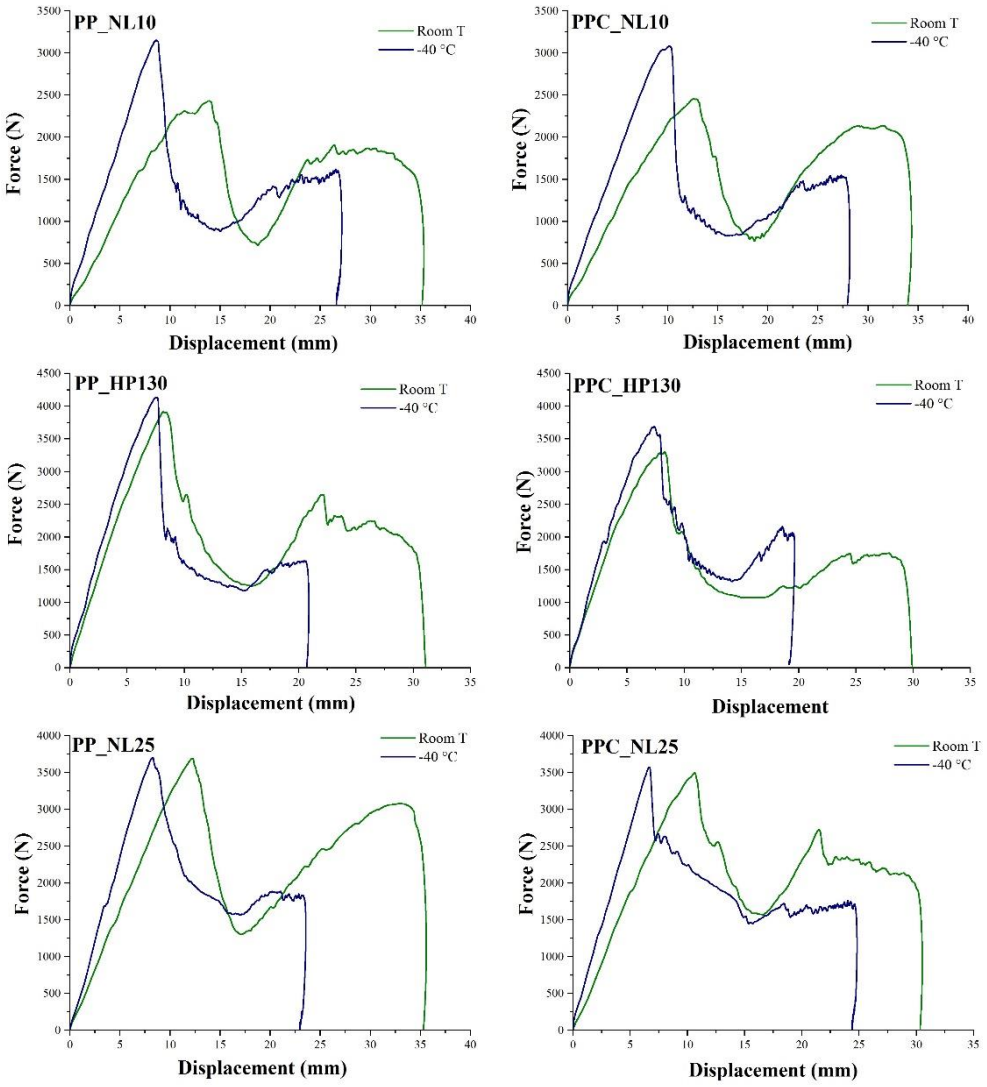


Figure 10: Low-velocity impact response curves of the six sandwich configurations at 75 % of perforation energy at room temperature and -40 °C

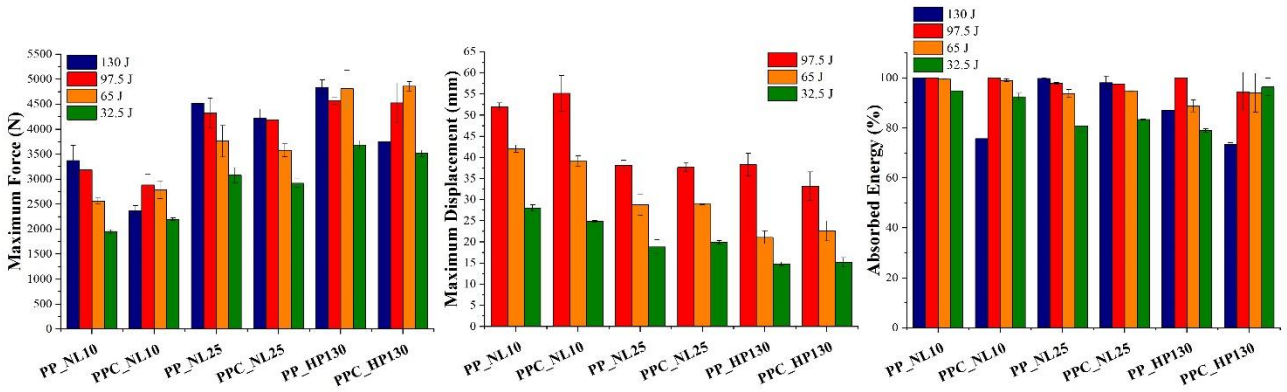


Figure 11: Maximum force, maximum displacement and absorbed energy of all six sandwich configurations tested at 60 °C and at 32.5 J, 65 J, 97.5 J and 130 J

This is not true for HP130 structures that, despite the improved matrix ductility, undergo perforation at 97.5 J with both PP and PPC skins. The higher stiffness of the polymeric core and its brittle behavior, due to its glass transition temperature higher than 60 °C, do not allow to reach high deformation in bending and to spread the impact load all over the sample thus inducing a stress concentration in the impacted zone. By the way, a certain improvement in the impact resistance thanks to the increased temperature can be observed even for this type of structures. Considering the data in Figure 11, all sandwich configurations are characterized by a decrease in maximum force, maximum displacement and percentage absorbed energy with decreasing impact energies. NL10 composites are characterized by the lowest maximum force and the highest maximum displacement due to the lowest stiffness of the overall structure whereas NL25 and HP130 ones display comparable results but a completely different damage mode. PP structures produced with agglomerated cork cores display a negligible indentation for each impact energy and almost a constant spacing of the skin meaning that the residual flexural properties of the structures should not be affected significantly. This is not true for PP HP130 structures that undergo perforation at both 130 J and 97.5 J thus suffering a sharp reduction in their load bearing capability. Similar conclusion can be drawn for PPC composites where the stress concentration suffered by HP130 sandwich structures leads to a severe indentation even at 65 J and 32.5 J. The more brittle behavior of PPC skins due to the improved fiber-matrix interface causes a relevant damage even in agglomerated cork structures but only until 97.5 J, as at 65 J and 32.5 J the excellent damping capabilities of cork allow to prevent core penetration.

## 4 CONCLUSIONS

The present work addressed the effect of operating temperature, i.e. -40 °C, room temperature and 60 °C, on the low-velocity impact response of bio-based sandwich structures produced with an agglomerated cork core and an intraply flax/basalt hybrid fabric as skin reinforcement. Moreover, well-established PVC foams were employed as benchmark to disclose potential advantages and drawbacks of the natural cores selected. The low-velocity impact campaign allowed to draw some important conclusions:

- A decrease in operating temperature plays an embrittlement effect on both natural and synthetic cores leading to a more extended crack on sample back side;
- Agglomerated cork critical point is the weak polymeric binder-cork granules interface responsible for the premature detachment of cork conical plugs that prevent the exploitation of its energy absorbing capabilities. The situation worsens at -40 °C where the polymeric binder reaches its glass transition and at 60 °C where it experiences a significant softening, leading to a reduction in the perforation threshold;
- The improved fiber-matrix interface provided by the maleic anhydride coupling agent plays a negative effect on laminates impact resistance, promoting a brittle behavior and hindering some energy dissipation mechanisms. The discrepancy between the two skins types is maximum at 60 °C where an increase of 20 J in non-compatibilized skins perforation energy is observed;
- NL10 structures are characterized by the same perforation energy of HP130 structures at -40 °C, a perforation threshold 5 J higher for PPC but 15 J lower for PP composites at room temperature and a more than 30 J higher perforation energy for PPC and more than 80 J for PP composites at 60 °C. NL25 structures are always characterized by an impact resistance higher than HP130 one: a 20 J and 10 J higher perforation energy at room temperature and at -40 °C, respectively, and a more than 30 J higher perforation energy for PPC and more than 80 J for PP composites at 60 °C;
- In addition to the improved impact resistance, agglomerated cork structures are able to provide a lower concentration of the damage and a lower permanent indentation;
- NL10 sandwich structures (450 kg/m$^3$) are able to provide an impact resistance perfectly comparable with HP130 one (425 kg/m$^3$), with an increase of only 5 % in structures weight and ensuring a partial

biodegradability of the component at the end of its life cycle. Unfortunately, their flexural performance is far from HP130 ones and this bio-based solution is valid only if impact resistance is one of the main design parameters and environmental sustainability must be favored with respect to the flexural properties.

- NL25 composites (540 kg/m$^3$) are characterized by an improved impact resistance and damage tolerance and by a flexural behavior closer to HP130 ones. The only drawback is an increase of 20 % in structure weight, but agglomerated cork NL25 is absolutely a feasible and valid alternative to HP130 to obtain a bio-based sandwich structure with an improved impact resistance, damage tolerance, dimensional stability and eco-compatibility for all those applications that can tolerate a slight increase in structure weight.

**Conflicts of Interest:** The Authors declare that there is no conflict of interest

**REFERENCES**


[1] Vinson R. J. The behavior of sandwich structures of isotropic and composite materials. Technomic publishing CO.,INC.; 1999.

[2] Olsson R. Engineering Method for Prediction of Impact Response and Damage in Sandwich Panels. J Sandw Struct Mater 2002;4. doi:10.1106/109963602023192.

[3] Olsson R. Methodology for predicting the residual strength of impacted sandwich panels. 1997.

[4] Chai GB, Zhu S. A review of low-velocity impact on sandwich structures. Proc Inst Mech Eng Part L J Mater Des Appl 2011;225:207–30. doi:10.1177/1464420711409985.

[5] Abrate S. Localized impact on sandwich structures with laminated facings. Appl Mech Rev 1997;50.

[6] Feng D, Aymerich F. Damage prediction in composite sandwich panels subjected to low-velocity impact. Compos Part A 2013;52:12–22. doi:10.1016/j.compositesa.2013.04.010.

[7] Mohmmed R, Ahmed A, Elgalib MA, Ali H. Low Velocity Impact Properties of Foam Sandwich Composites : A Brief Review. Int J Eng Sci Innov Technol 2014;3:579–91.

[8] Xue X, Zhang C, Chen W, Wu M, Zhao J. Study on the impact resistance of honeycomb sandwich structures under low-velocity / heavy mass. Compos Struct 2019;226:111223. doi:10.1016/j.compstruct.2019.111223.

[9] Hazizan MA, Cantwell WJ. The low velocity impact response of foam-based sandwich structures. Compos Part B Eng 2002;33:193–204. doi:10.1016/j.compscitech.2012.07.006.

[10] Caprino G, Teti R. Impact and post-impact behavior of foam core sandwich structures. Compos Struct 1994;29:47–55.

[11] Schubel PM, Luo JJ, Daniel IM. Impact and post impact behavior of composite sandwich panels. Compos Part A Appl Sci Manuf 2007;38:1051–7. doi:10.1016/j.compositesa.2006.06.022.

[12] Pereira H. The rationale behind cork properties: A review of structure and chemistry. BioResources 2015;10:1–23. doi:10.15376/biores.10.3.Pereira.

[13] Jardin RT, Fernandes FAO, Pereira AB, Alves de Sousa RJ. Static and dynamic mechanical response of different cork agglomerates. Mater Des 2015;68:121–6. doi:10.1016/j.matdes.2014.12.016.

[14] Thomas S, Paul SA, Pothan LA, Deepa B. Natural Fibres : Structure , Properties and Applications. Cellul. Fibers Bio- Nano-Polymer Compos., 2011, p. 3–42. doi:10.1007/978-3-642-17370-7.

[15] Fiore V, Scalici T, Di Bella G, Valenza A. A review on basalt fibre and its composites. Compos Part B Eng 2015;74:74–94. doi:10.1016/j.compositesb.2014.12.034.

[16] Ralph C, Lemoine P, Archer E, Mcilhagger A. Mechanical properties of short basalt fibre reinforced polypropylene and the effect of fibre sizing on adhesion. Compos Part B 2019;176.

doi:10.1016/j.compositesb.2019.107260.
[17] Lilli M, Sarasini F, Di Fausto L, González C, Fernández A, Lopes CS, et al. Chemical Regeneration of Thermally Conditioned Basalt Fibres. Appl Sci 2020;10. doi:10.3390/app10196674.
[18] Baran I, WeiJermars W. Residual bending behaviour of sandwich composites after impact. J Sandw Struct Mater 2018:1–21. doi:10.1177/1099636218757164.
[19] Atas C, Sevim C. On the impact response of sandwich composites with cores of balsa wood and PVC foam. Compos Struct 2010;93:40–8. doi:10.1016/j.compstruct.2010.06.018.
[20] Daniel IM, Abot JL, Schubel PM, Luo J. Response and Damage Tolerance of Composite Sandwich Structures under Low Velocity Impact. Exp Mech 2012;52:37–47. doi:10.1007/s11340-011-9479-y.
[21] Arteiro A, Reis ALMA, Nóvoa PJRO, Silva LFM, Zupan M, Marques AT. Low velocity impact and flexural performance of sandwich structures with cork and polymer foam cores. Cienc e Tecnol Dos Mater 2013;25:79–84. doi:10.1016/j.ctmat.2014.03.003.
[22] Wang H, Ramakrishnan KR, Shankar K. Experimental study of the medium velocity impact response of sandwich panels with different cores. Mater Des 2016;99:68–82. doi:10.1016/j.matdes.2016.03.048.
[23] Castro O, Silva JM, Devezas T, Silva A, Gil L. Cork agglomerates as an ideal core material in lightweight structures. Mater Des 2010;31:425–32. doi:10.1016/j.matdes.2009.05.039.
[24] Hachemane B, Zitoune R, Bezzazi B, Bouvet C. Sandwich composites impact and indentation behaviour study. Compos Part B Eng 2013;51:1–10. doi:10.1016/j.compositesb.2013.02.014.
[25] Silva JM, Nunes CZ, Franco N, Gamboa P V. Damage tolerant cork based composites for aerospace applications. Aeronaut J 2011;115:567–75. doi:10.1017/S0001924000006205.
[26] Múgica JI, Aretxabaleta L, Ulacia I, Aurrekoetxea J. Impact characterization of thermoformable fibre metal laminates of 2024-T3 aluminium and AZ31B-H24 magnesium based on self-reinforced polypropylene. Compos Part A 2014;61:67–75. doi:10.1016/j.compositesa.2014.02.011.
[27] Sayer M, Bektaş NB, Sayman O, Topçu M. An Experimental Investigation on the Impact Behaviour of Glass / Epoxy and Hybrid Composite Plates. Adv Compos Lett 2009;18:113–22. doi:10.1177/096369350901800401.
[28] Sergi C, Tirillò J, Sarasini F, Barbero Pozuelo E, Sanchez-Saez S, Burgstaller C. The Potential of Agglomerated Cork for Sandwich Structures : A Systematic Investigation of Physical , Thermal , and Mechanical Properties. Polymers (Basel) 2019;11.
[29] Paiva D, Magalhães FD. Dynamic mechanical analysis and creep-recovery behavior of agglomerated cork. Eur J Wood Wood Prod 2017. doi:10.1007/s00107-017-1158-y.
[30] Simeoli G, Sorrentino L, Touchard F, Mellier D, Oliviero M, Russo P. Comparison of falling dart and Charpy impacts performances of compatibilized and not compatibilized polypropylene / woven glass fibres composites. Compos Part B 2019;165:102–8. doi:10.1016/j.compositesb.2018.11.090.
[31] Sorrentino L, Simeoli G, Iannace S, Russo P. Mechanical performance optimization through interface strength gradation in PP / glass fi bre reinforced composites. Compos Part B 2015;76:201–8. doi:10.1016/j.compositesb.2015.02.026.
[32] Boccardi S, Meola C, Carlomagno GM, Sorrentino L, Simeoli G, Russo P. Effects of interface strength gradation on impact damage mechanisms in polypropylene / woven glass fabric composites. Compos Part B 2016;90:179–87. doi:10.1016/j.compositesb.2015.12.004.
[33] Dong Z, Ding R, Zheng L, Zhang X, Yu C. Thermal Properties of Flax Fiber Scoured by Different Methods. Therm Sci 2015;19:939–45. doi:10.2298/TSCI130329005Z.
[34] Khalfallah M, Abbès B, Abbès F, Guo YQ, Marcel V, Duval A, et al. Innovative flax tapes reinforced Acrodur biocomposites : A new alternative for automotive applications. Mater Des 2014;64:116–26. doi:10.1016/j.matdes.2014.07.029.